Slip Effect on Stagnation Point Flow past a Stretching Surface with the Presence of Heat Generation/Absorption and Newtonian Heating

Muhammad Khairul Anuar Mohamed[1], Nor Aida Zuraimi Md Noar[2], Zulkhibri Ismail[3], Abdul Rahman Mohd Kasim[4], Norhafizah Md Sarif[5], Mohd Zuki Salleh[6,*], Anuar Ishak[7]

[1,2,3,4,5,6]Applied & Industrial Mathematics Research Group,
Faculty of Industrial Science and Technology,
Universiti Malaysia Pahang, 26300 UMP Kuantan, Pahang, MALAYSIA.
[7]School of Mathematical Sciences, Faculty of Science & Technology,
Universiti Kebangsaan Malaysia,
43600 UKM Bangi, Selangor, MALAYSIA.

Corresponding author*: zukikuj@yahoo.com
[1]baa_khy@yahoo.com, [2]aidaz@ump.edu.my, [3]zulkhibri@ump.edu.my, [4]rahman@ump.edu.my,
[5]norhafizah@ump.edu.my, [7]anuar_mi@ukm.edu.my

Abstract. Present study solved numerically the velocity slip effect on stagnation point flow past a stretching surface with the presence of heat generation/absorption and Newtonian heating. The governing equations which in the form of partial differential equations are transformed to ordinary differential equations before being solved numerically using the Runge-Kutta-Fehlberg method in MAPLE. The numerical solution is obtained for the surface temperature, heat transfer coefficient, reduced skin friction coefficient as well as the temperature and velocity profiles. The flow features and the heat transfer characteristic for the pertinent parameter such as Prandtl number, stretching parameter, heat generation/absorption parameter, velocity slip parameter and conjugate parameter are analyzed and discussed.

INTRODUCTION

Stagnation point flow can be describe as the fluid motion acted perpendicular to the surface for example the flat plate, cylinder or sphere then flowing symmetrical horizontally to the surface. This flow movement called as the stagnation line [1]. Classical study regarding to this problem is from Hiemenz [2] who developed the similarity solution for the governing Navier-Stokes equations. Eckert [3] then reported the similarity solutions for the energy equations.

In considering the heat transfer on a stretching surface, this configuration is important in many industrial manufacturing processes especially in a production of sheeting material. The processes of paper, rubber and plastic sheet, tire production, glass blowing and continuous casting usually involved the hot molten phase with some stretching effect. In order to cooling down the product, it is surrounding by the fluid motion which promoted to a convective heat transfer process [4]. The quality of the final product will depends on the rate of the heat transfer at the stretching surface [5].

The study on this topic received a researcher's attention since 45 years ago. Crane [6] considered the boundary layer flow over a stretching sheet before Gupta and Gupta [7] updated it with suction and blowing effect. Due to the arises of industrial and engineering, this study was extended to viscoelastic fluid, micropolar fluid, nanofluid, Williamson fluid, power-law fluid and other non-Newtonian fluid by many investigators including Nazar et al. [8], Ishak et al. [9], Chen [10], Abbas et al. [11], Bachok et al. [12], Hayat et al. [13] and recently by Mohamed et al. [14].

Slip condition simplified as the condition where the fluid flow come in contact with surface have relative velocity thus disobeyed the no slip condition. Ariel et al. [15] consider a partial slip effects on the viscoelastic fluid flow past a stretching sheet. The Walter's liquid-B model is considered with discussing is detail regarding the behavior of skin friction coefficient. Next, Aman et al. [16] applied a slip effects on mixed convection near the stagnation point on a vertical surface. Both velocity and thermal slip is considered. It is found that the velocity slip increases the heat transfer rate at the surface, while the thermal slip decreases it. Recent studies on slip including the works by Hashim et al. [17], Mohamed et al. [18] and Noor et al. [19] who consider the effects of slip and partial slip on the stagnation point flow over a stretching sheet embedded in viscoelastic fluid and micropolar nanofluid with viscous dissipation and convective boundary conditions, respectively.

Motivated from the above literature, present study consider the velocity slip effect on stagnation point flow past a stretching surface with the presence of heat generation/absorption and Newtonian heating. The results obtained in this study are important for researchers in this area either in numerical or experimental approach so it can be used as a comparison and reference in future.

MATHEMATICAL FORMULATIONS

A steady two-dimensional stagnation-point flow over a heated stretching/shrinking plate immersed in an incompressible viscous fluid of ambient temperature, T_∞ is considered. The external velocity $u_e(x)$ and the stretching velocity $u_w(x)$ are assumed linear and in the forms of $u_e(x)=ax$ and $u_w(x)=bx,$ respectively. Note that *a* and *b* are constants. The physical models of the coordinate system are shown in Fig. 1. According to Salleh et al. [1] and Mohamed et al. [20], the boundary layer equations governed the model are:

$$\frac{\partial u}{\partial x}+\frac{\partial v}{\partial y}=0 \tag{1}$$

$$u\frac{\partial u}{\partial x}+v\frac{\partial u}{\partial y}=u_e\frac{du_e}{dx}+\nu\frac{\partial^2 u}{\partial y^2} \tag{2}$$

$$u\frac{\partial T}{\partial x}+v\frac{\partial T}{\partial y}=\alpha\frac{\partial^2 T}{\partial y^2}+\frac{Q_o}{\rho C_p}\left(T-T_\infty\right) \tag{3}$$

subject to the boundary conditions

$$u=u_w(x)+\gamma^*\mu\frac{\partial u}{\partial y},\ \ v=0,\ \ \frac{\partial T}{\partial y}=-h_sT \ \text{ at } \ y=0,$$

$$u=u_e(x),\ \ T\to T_\infty \ \text{ as } \ y\to\infty, \tag{4}$$

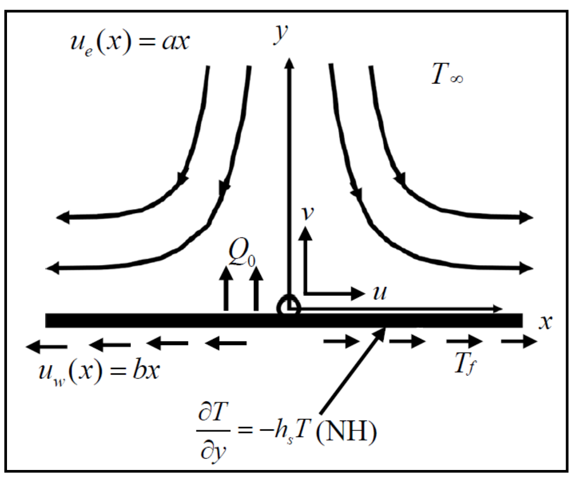

FIGURE 1. The physical model of coordinate system

where *u* and *v* are the velocity components along the *x* and *y* directions, respectively. Further, *T* is the fluid temperature in the boundary layer, ν is the kinematic viscosity, α is the thermal diffusivity, Q_o is the dimensional heat generation or absorption coefficient, ρ is fluid density, C_p is the specific heat, μ is dynamic viscosity, $\beta *$ is the velocity slip factor and h_s is the heat transfer coefficient. Next, it is introduce the similarity variables:

$$\eta = \left(\frac{u_e}{\nu x}\right)^{1/2} y, \quad \psi = \left(\nu x u_e\right)^{1/2} f(\eta), \quad \theta(\eta) = \frac{T - T_\infty}{T_\infty}, \tag{5}$$

where ψ is the stream function defined as $u = \frac{\partial \psi}{\partial y}$ and $v = -\frac{\partial \psi}{\partial x}$, which identically satisfies (1). Thus, the term u and v are calculated as follows:

$$u = axf'(\eta), \; v = -(a\nu)^{1/2} f(\eta), \tag{6}$$

where prime denotes differentiation with respect to η. By substituting (5) and (6) into (2) and (3), then the following nonlinear ordinary differential equations are obtained:

$$f''' + ff'' + 1 - f'^2 = 0 \tag{7}$$

$$\frac{1}{\Pr}\theta'' + f\theta' + \lambda\theta = 0 \tag{8}$$

where $\Pr = \frac{\nu}{\alpha}$ is the Prandtl number and $\lambda = \frac{Qo}{b\rho C_p}$ is the heat generation $(\lambda > 0)$ or absorption $(\lambda < 0)$. The boundary conditions (4) become

$$\begin{gathered} f(0) = 0, \;\; f'(0) = \varepsilon + \beta f''(0), \;\; \theta'(0) = -\gamma(1 + \theta(0)), \\ f'(\eta) \to 1, \;\; \theta(\eta) \to 0, \;\; \text{as} \quad y \to \infty. \end{gathered} \tag{9}$$

$\varepsilon = \frac{b}{a}$ is a stretching parameter, $\beta = \beta * \rho\left(a\nu\right)^{1/2}$ is the velocity slip parameter and $\gamma = h_s\left(\frac{\nu}{a}\right)^{1/2}$ is the conjugate parameter. The physical quantities of interest are the surface temperature $\theta(0)$, the heat transfer coefficient $-\theta'(0)$ and the skin friction coefficient C_f which is given by

$$C_f = \frac{\tau_w}{\rho u_e^2}, \tag{10}$$

with $\tau_w = \mu\left(\frac{\partial u}{\partial y}\right)_{y=0}$ is the surface shear stress. Using the similarity variables in (5) gives

$$C_f \operatorname{Re}_x^{1/2} = f''(0), \tag{11}$$

where $\operatorname{Re}_x = \frac{u_e x}{\nu}$ is the local Reynolds number.

RESULTS AND DISCUSSION

Equations (7) and (8) with boundary conditions (9) were solved numerically using the Runge-Kutta_Fehlberg method which encoded in Maple software. Boundary layer thickness η_∞ in the range of 4 to 10 is sufficient to provide an asymptotic numerical result. Five variables considered which are the Prandtl number $\Pr$, the stretching parameter ε, the heat generation/absorption parameter λ, the velocity slip parameter β and the conjugate parameter γ. The $\Pr = 7$ (water) is used so that the calculation made in this study is based on the realistic incompressible viscous fluid. It is worth mentioning here that as $\varepsilon = \lambda = \beta = 0$, the case study were similar with those published by Salleh [21], therefore this can be used as comparison to validated the numerical computation used. Table 1 shows the comparison values of surface temperature $\theta(0)$ and the heat transfer coefficient $-\theta'(0)$ for various values of $\Pr$. It is found that the results are in a good agreement, thus gives a confidence in term of results obtained accuracy.

The values of $\theta(0)$ and $-\theta'(0)$ with various values of γ and λ are tabulated in Table 2. Noted that $\lambda > 0$ is the heat generation while $\lambda < 0$ for the heat absorption effect. From table it is found that the present of heat absorption reduce the values of $\theta(0)$ and $-\theta'(0)$. The situation goes contrary for the heat generation effects which gives the increase in both $\theta(0)$ and $-\theta'(0)$. This is physically realistic since the heat generation have rises the amount of heat at the plate and increase the surface temperature. From the numerical computation, it is suggested that the present of heat generation effect reduced the range of γ for which the solution exists. Further, the $\theta(0)$ and $-\theta'(0)$ increases with the increase of γ. The rise of $-\theta'(0)$ becomes more significant as γ increases.

TABLE 1. Comparison between the present solution with previously published results when $\gamma = 1$ and $\varepsilon = \lambda = \beta = 0$.

Pr	Salleh [21]		Mohamed et al. [20]		Present	
	$\theta(0)$	$-\theta'(0)$	$\theta(0)$	$-\theta'(0)$	$\theta(0)$	$-\theta'(0)$
5	23.0042	24.0042	23.0239	24.0239	23.0239	24.0239
7	5.6872	6.6872	5.6062	6.6062	5.6062	6.6062
10	2.9226	3.9226	2.9516	3.9516	2.9516	3.9516
100	0.6866	1.6866	0.5034	1.5034	0.5034	1.5034
1000	0.2593	1.2593	0.1809	1.1809	0.1809	1.1809

TABLE 2. Values of $\theta(0)$ and $-\theta'(0)$ for various values of γ and λ when $\beta = \varepsilon = 0.5$ and $\Pr = 7$.

γ	$\lambda = -0.3$		$\lambda = 0.0$		$\lambda = 0.3$	
	$\theta(0)$	$-\theta'(0)$	$\theta(0)$	$-\theta'(0)$	$\theta(0)$	$-\theta'(0)$
0.1	0.0450	0.1045	0.0563	0.1056	0.0804	0.1080
0.5	0.2741	0.6370	0.3630	0.6815	0.5930	0.7965
0.7	0.4310	1.0017	0.5945	1.1161	1.084	1.4619
1	0.75516	1.7552	1.1396	2.1396	2.9141	3.9141
1.5	1.8199	4.2298	3.9736	7.4604		
1.7	2.7234	6.3298	9.5780	17.9826		

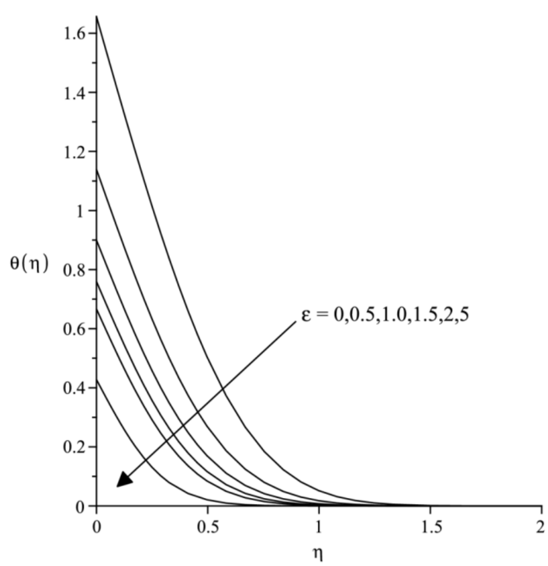

FIGURE 2. Temperature profiles $\theta(\eta)$ for various values of ε when $\Pr = 7, \beta = 0.5, \lambda = 0$ and $\gamma = 1$.

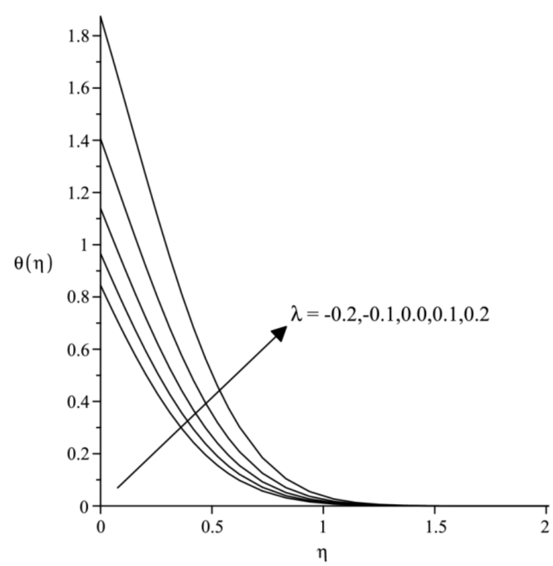

FIGURE 3. Temperature profiles $\theta(\eta)$ for various values of λ when $\Pr = 7, \beta = \varepsilon = 0.5$ and $\gamma = 1$.

Figures 2-5 illustrated the temperature profiles for various values of $\varepsilon, \lambda, \beta$ and γ, respectively. In Fig. 2, it is found that the increase in ε gives a reduction in both surface temperature as well as its thermal boundary layer thickness. Domination of stretching velocity over the external velocity has reduced the energy ability thus prevent the energy from spread up, thus reduced the thermal boundary layer thickness. Meanwhile, the increase of both λ and γ results to the increase in surface temperature and thermal boundary layer thickness. This may be explained as follows; the present of heat generation have increase the temperature at the surface and therefore increase the energy in the boundary layer. Therefore, the capability in energy transferring increases thus allowed the energy to spread up away from the boundary layer which thickening the thermal boundary layer. The temperature profiles for both parameters are plotted in Figs. 3 and 4, respectively.

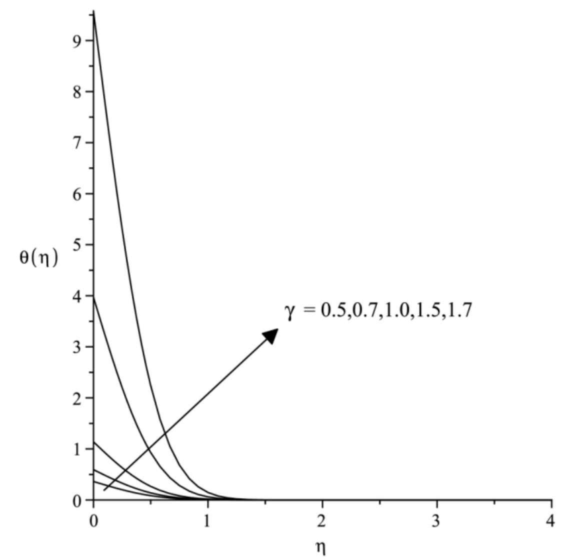

FIGURE 4. Temperature profiles $\theta(\eta)$ for various values of γ when $\Pr = 7, \beta = \varepsilon = 0.5$ and $\lambda = 0$.

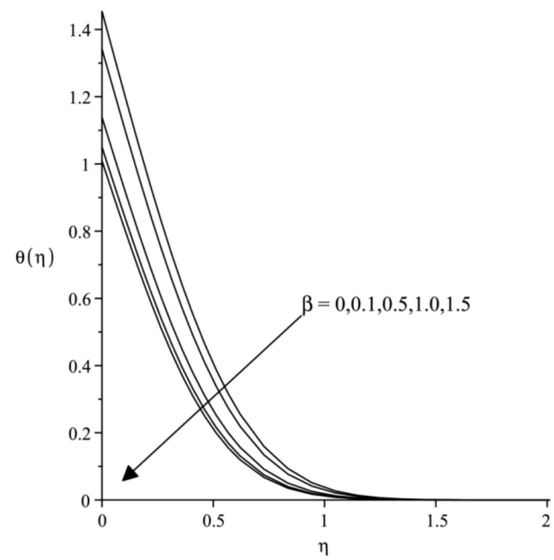

FIGURE 5. Temperature profiles $\theta(\eta)$ for various values of β when $\Pr = 7, \varepsilon = 0.5, \lambda = 0$ and $\gamma = 1$.

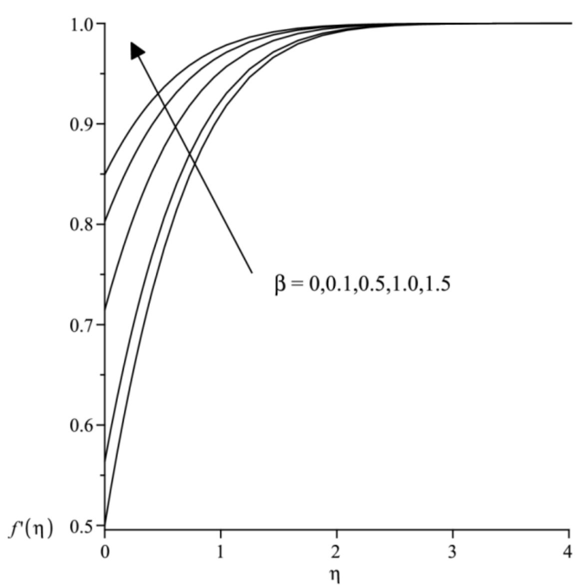

FIGURE 6. Velocity profiles $f'(\eta)$ for various values of β when $\Pr = 7, \varepsilon = 0.5, \lambda = 0$ and $\gamma = 1$.

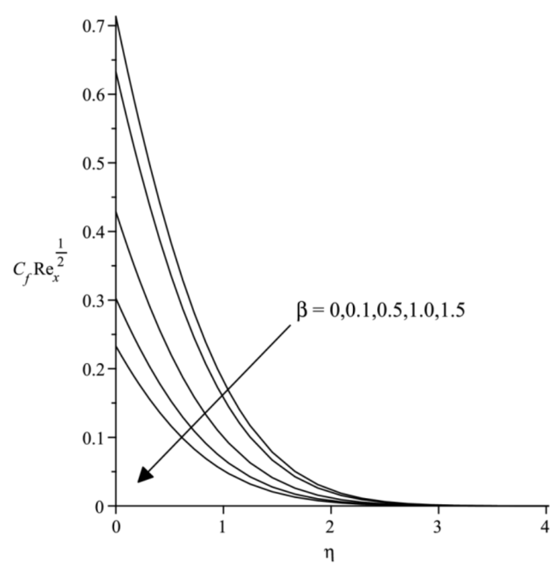

FIGURE 7. Skin friction coefficient $C_f \mathrm{Re}_x^{1/2}$ for various values of β when $\Pr = 7, \varepsilon = 0.5, \lambda = 0$ and $\gamma = 1$.

In Fig. 5, the increase of β gives a reduction in $\theta(0)$. It is observed that the reduction in $\theta(0)$ becoming less significant for high value of β. This is physically sign that slightly velocity slip effect (small β) is enough to influence the value of $\theta(0)$. In considering the thickness of thermal boundary layer, it is found that β gives only a small reduction on the thermal boundary layer thicknesses.

On the other hand, β gives more significant effects onto velocity thermal boundary layer thickness and its velocity profiles as shown in Fig. 6. For the case of stretching velocity is half from the external velocity $(\varepsilon = 0.5)$, the increase of β gives a rise in velocity profiles but the boundary layer thickness decreases. The presence of β has accelerate the fluid flow thus reduce the deficit between the velocity of ambient flow with the velocity inside the boundary layer. This situation gives an impact on the velocity gradient thus reduced the skin friction coefficient $C_f \mathrm{Re}_x^{1/2}$ as shown in Fig. 7. In real world application, the velocity slip effect alone is efficient to reduce the skin friction which contributed to less erosion onto component which prolonged the lifetime.

Next, Fig. 8 show the variation of $C_f \mathrm{Re}_x^{1/2}$ for various values of ε. It is found that $C_f \mathrm{Re}_x^{1/2}$ is a decreasing function. When β is absent $(\beta = 0.0)$, the value of $C_f \mathrm{Re}_x^{1/2}$ decrease drastically as ε increases. In the presence of β $(\beta = 0.5)$, the reducing in $C_f \mathrm{Re}_x^{1/2}$ is less abrupt. From figure, the intersection point between curves occur at $\varepsilon = 1$ which illustrated that the velocity slip effect is dominant on $C_f \mathrm{Re}_x^{1/2}$ for $\varepsilon > 1$ while the opposite trends occur for $\varepsilon < 1$.

Lastly, the variation of $\theta(0)$ for various values of ε and λ are plotted in Figs. 9 and 10, respectively. In Fig. 9, for $\varepsilon < 1$, the absence of β gives higher $\theta(0)$ compared to $\beta = 0.5$. This situation change for $\varepsilon > 1$ where the presence of β gives a slightly increment in $\theta(0)$. Further, it is found that the $\theta(0)$ decreases along ε. Contrary with Fig. 10, the $\theta(0)$ is an increasing function with λ. The presence of heat generator $(\lambda > 0)$ results to a drastic increases in $\theta(0)$. From figure, it is observed that too much in heat generator will interrupt the convection heat transfer process which represented as non acceptable solution. To get a physically acceptable solution, λ must be lower than or equal to its critical value; $\lambda_{c1} = 0.3404$ for $\beta = 0.0$ and $\lambda_{c2} = 0.4605$ for $\beta = 0.5$. It is suggested that the presence of β enhanced the range of λ for which the solution exists.

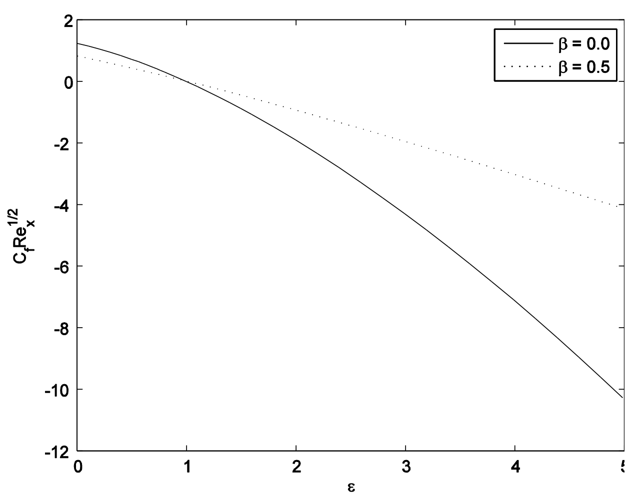

FIGURE 8. Variation of $C_f \mathrm{Re}_x^{1/2}$ for various values of ε when $\mathrm{Pr} = 7, \lambda = 0$ and $\gamma = 1$.

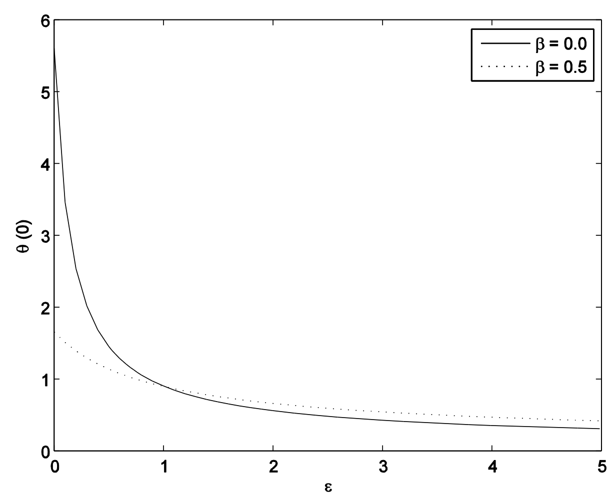

FIGURE 9. Variation of $\theta(0)$ for various values of ε when $\mathrm{Pr} = 7, \lambda = 0$ and $\gamma = 1$.

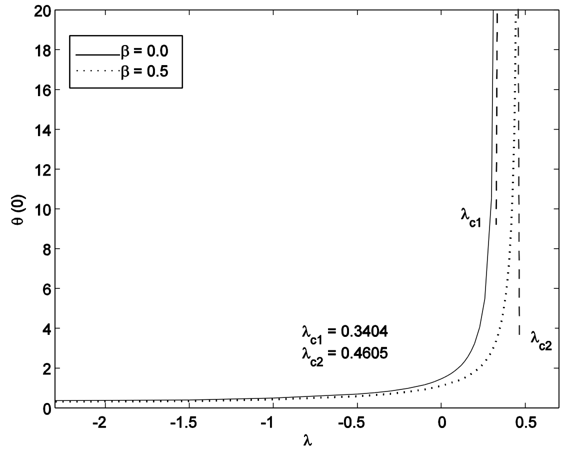

FIGURE 10. Variation of $\theta(0)$ for various values of λ when $\Pr = 7, \beta = \varepsilon = 0.5$ and $\gamma = 1$.

CONCLUSIONS

As a conclusion, the increase of stretching parameter and velocity slip parameter results to a decreasing in surface temperature and thermal boundary layer thickness. Meanwhile, the effect of heat generation/absorption parameter and conjugate parameter does oppositely.

Next, it is found that the presence of velocity slip parameter reduce a stretching parameter effect on skin friction coefficient. The skin friction coefficient decreases less with the presence of the velocity slip parameter.

Lastly, it is suggested that to get a physically acceptable solution, the value of heat generation/absorption parameter must be less than or equal to its critical value. From the numerical computation, the presence of velocity slip parameter rise the critical value which enhanced the range of solution exists.

ACKNOWLEDGMENTS

The authors would like to thank the Universiti Malaysia Pahang for the financial and moral support in the form of research grant RDU140111 and RDU150101

REFERENCES

1. M. Z. Salleh, R. Nazar and I. Pop, *Chemical Engineering Communications* **196**, 987-996 (2009).
2. K. Hiemenz, *Dingley's Polytechnic Journal* **32**, 321-410 (1911).
3. E. R. G. Eckert, *VDI Forsch.* **461** (1942).
4. R. Nazar, N. Amin, D. Filip and I. Pop, *International journal of engineering science* **42**(11), 1241-1253 (2004).
5. N. M. Sarif, M. Z. Salleh and R. Nazar, *Procedia Engineering* **53**(0), 542-554 (2013).
6. L. J. Crane, *Zeitschrift für Angewandte Mathematik und Physik.* **21**, 645-647 (1970).
7. P. S. Gupta and A. S. Gupta, *The Canadian Journal of Chemical Engineering* **55**(6), 744-746 (1977).
8. R. Nazar, N. Amin, D. Filip and I. Pop, *International Journal of Non-Linear Mechanics* **39**(7), 1227-1235 (2004).
9. A. Ishak, R. Nazar and I. Pop, *Meccanica* **43**(4), 411-418 (2008).
10. C. H. Chen, *International Journal of Non-Linear Mechanics* **44**(6), 596-603 (2009).
11. Z. Abbas, Y. Wang, T. Hayat and M. Oberlack, *Nonlinear Analysis: Real World Applications* **11**(4), 3218-3228 (2010).
12. N. Bachok, A. Ishak and I. Pop, *Nanoscale Res. Lett.* **6** (2011).
13. T. Hayat, Z. Iqbal and M. Mustafa, *Journal of Mechanics* **28**(01), 209-216 (2012).

14. M. K. A. Mohamed, N. A. Z. Noar, M. Z. Salleh and A. Ishak, *AIP Conference Proceedings* **1643**, 635-641 (2015).
15. P. Ariel, T. Hayat and S. Asghar, *Acta Mechanica* **187**(1-4), 29-35 (2006).
16. F. Aman, A. Ishak and I. Pop, *Applied Mathematics and Mechanics* **32**(12), 1599-1606 (2011).
17. H. Hashim, M. K. A. Mohamed, A. Hussanan, N. Ishak, N. M. Sarif and M. Z. Salleh, *AIP Conference Proceedings* **1691**, 040007 (2015).
18. M. K. A. Mohamed, M. Z. Salleh, A. Ishak and I. Pop, *The European Physical Journal Plus* **130**(8), 1-9 (2015).
19. N. F. M. Noor, R. U. Haq, S. Nadeem and I. Hashim, *Meccanica* **50**(8), 2007-2022 (2015).
20. M. K. A. Mohamed, M. Z. Salleh, R. Nazar and A. Ishak, *Sains Malaysiana* **41**(11), 1467-1473 (2012).
21. M. Z. Salleh, "Pemodelan Matematik bagi Aliran Lapisan Sempadan Olakan dengan Pemanasan Newtonan," Tesis Dr. Falsafah, Universiti Kebangsaan Malaysia, 2011.